Scientific Report

TRANSPARENT PROCESS

EMBO reports

Intellectual disability-associated dBRWD3 regulates gene expression through inhibition of HIRA/YEM-mediated chromatin deposition of histone H3.3

Wei-Yu Chen[1,†], Hsueh-Tzu Shih[1,†], Kuei-Yan Liu[1], Zong-Siou Shih[1], Li-Kai Chen[1], Tsung-Han Tsai[1], Mei-Ju Chen[2], Hsuan Liu[3,4], Bertrand Chin-Ming Tan[4,5], Chien-Yu Chen[6], Hsiu-Hsiang Lee[1], Benjamin Loppin[7], Ounissa Aït-Ahmed[8] & June-Tai Wu[1,9,10,*]

Abstract

Many causal mutations of intellectual disability have been found in genes involved in epigenetic regulations. Replication-independent deposition of the histone H3.3 variant by the HIRA complex is a prominent nucleosome replacement mechanism affecting gene transcription, especially in postmitotic neurons. However, how HIRA-mediated H3.3 deposition is regulated in these cells remains unclear. Here, we report that *dBRWD3*, the *Drosophila* ortholog of the intellectual disability gene *BRWD3*, regulates gene expression through H3.3, HIRA, and its associated chaperone Yemanuclein (YEM), the fly ortholog of mammalian Ubinuclein1. In *dBRWD3* mutants, increased H3.3 levels disrupt gene expression, dendritic morphogenesis, and sensory organ differentiation. Inactivation of *yem* or *H3.3* remarkably suppresses the global transcriptome changes and various developmental defects caused by *dBRWD3* mutations. Our work thus establishes a previously unknown negative regulation of H3.3 and advances our understanding of BRWD3-dependent intellectual disability.

Keywords BRWD3; HIRA; histone H3.3; intellectual disability; YEM
Subject Categories Chromatin, Epigenetics, Genomics & Functional Genomics; Neuroscience; Development & Differentiation
DOI 10.15252/embr.201439092 | Received 23 May 2014 | Revised 15 January 2015 | Accepted 16 January 2015 | Published online 9 February 2015
EMBO Reports (2015) 16: 528–538

Introduction

Genomic DNA is wrapped around histone octamers and organized into chromatin. The dynamic chromatin structures instruct how a gene should be transcribed during developmental processes. Information associated with chromatin structure can be established and edited by at least four categories of epigenetic mechanisms: DNA methylation, histone tail modifications, nucleosome remodeling, and exchanges of histone variants. Among histone variants, the histone H3 variant H3.3 differs from the conventional histone H3.1 by only 5 residues, but has distinct deposition mechanisms and biological functions. Deposition of H3.3-containing nucleosomes is mediated by Daxx/ATRX or HIRA complex throughout the cell cycle (replication independent), whereas deposition of H3.1 into chromatin is mediated by histone chaperone CAF-1 mainly during DNA replication (replication dependent) [1]. HIRA and its associated chaperone Yemanuclein (YEM), the fly ortholog of mammalian Ubinuclein1, deposit H3.3 to actively transcribed regions, nucleosome-free gaps [2,3] and the male pronucleus at fertilization [4–7]. In contrast, the Daxx/ATRX complex deposits H3.3 to the telomeres [8–10]. During development, deposition of H3.3 but not H3.1 establishes the epigenetic memory of an active gene state [11]. Because H3.3 deposition is associated with gene transcription [12,13] and enriched over actively transcribed regions [8,14], it has been assumed that H3.3 could promote gene transcription. However, HIRA/YEM-mediated H3.3 deposition at the promoter regions was also shown to be required for PRC2 recruitment and bivalent gene silencing [15]. Although the diverse roles of HIRA and H3.3 on gene activation and repression have been studied extensively, how

1 Institute of Molecular Medicine, College of Medicine, National Taiwan University, Taipei, Taiwan
2 Genome and Systems Biology Degree Program, National Taiwan University and Academia Sinica, Taipei, Taiwan
3 Department of Cell and Molecular Biology, College of Medicine, Chang Gung University, Tao-Yuan, Taiwan
4 Molecular Medicine Research Center, Chang Gung University, Tao-Yuan, Taiwan
5 Department of Biomedical Sciences and Graduate Institute of Biomedical Sciences, College of Medicine, Chang Gung University, Tao-Yuan, Taiwan
6 Bio-Industrial Mechatronics Engineering, National Taiwan University, Taipei, Taiwan
7 Centre de Génétique et de Physiologie Moléculaire et Cellulaire, CNRS UMR5534, Université Claude Bernard Lyon 1, Villeurbanne, France
8 Institute of Regenerative medicine and Biotherapy (IRMB), Inserm U1203, Saint-Eloi Hospital, CHRU Montpellier, France
9 Department of Dermatology, National Taiwan University Hospital and National Taiwan University College of Medicine, Taipei, Taiwan
10 Research Center for Developmental Biology and Regenerative Medicine, National Taiwan University, Taipei, Taiwan
*Corresponding author. Tel: +886 2 23123456 ext 88367; E-mail: junetai.wu@gmail.com
†These authors contributed equally to this work

HIRA/YEM-mediated deposition of H3.3 is regulated remains unknown.

Early-onset cognitive impairment, known as mental retardation or intellectual disability (ID), is defined as a reduced ability to learn new skills [16]. Genetic studies suggest that ID is a disease of heterogeneous causes. For instance, in X-linked ID (XLID), which accounts for 10-12% of all forms of ID, the biological functions of the causative genes are diverse and not restricted to neurons [17]. Among the XLID causative genes, *CUL4B* encodes the scaffold component of cullin-RING E3 ligase, CRL4B [18,19]. Like other CRL ubiquitin E3 ligases, CRL4B can ubiquitinate different substrates by incorporating a distinct substrate receptor through DDB1 (DNA damage-binding protein 1) [20]. Interestingly, one of the CRL4 substrate receptors, *BRWD3* (Bromodomain and WD repeat-containing protein 3), was mutated in three XLID families [21,22]. These genetic studies suggest that a BRWD3-containing CRL4 complex is critical for maintaining neural functions and structures. How the BRWD3-containing CRL4 complex functions in the nervous system is not known. Here, we report that dBRWD3, the fly homolog of XLID protein BRWD3, negatively regulates the amount of H3.3 associated with YEM and the levels of chromatin-associated H3.3. Strikingly, the diverse transcriptome changes and developmental defects found in *dBRWD3* mutants were restored to normal by inactivation of the HIRA/YEM–H3.3 pathway. These findings identify dBRWD3 as a negative regulator of the HIRA/YEM–H3.3 pathway and provide a potential molecular mechanism underlying the X-linked intellectual disability.

Results and Discussion

dBRWD3 regulates photoreceptor differentiation

To explore the molecular function of BRWD3 that underlies its implication in intellectual disability, we characterized *dBRWD3*, an essential gene encoding the only BRWD family protein in *Drosophila* [23]. By immunofluorescence analysis, we confirmed that dBRWD3 protein is absent in the molecularly null *dBRWD3* mutant, as previously reported [23] (Supplementary Fig S1A, dashed lines). In *dBRWD3* mutant clones, the photoreceptors projected axons to brain normally (Fig 1A, arrows, $n = 52$, penetrance = 100%), but did not differentiate into mature neurons expressing Chaoptin, a terminal differentiation marker (Fig 1B, dashed lines, $n = 56$, penetrance = 92.9%). The expression of Prospero, a homeobox protein, was also markedly reduced in the mutant clones, indicating that the differentiation of R7 and cone cells is arrested (Fig 1C, dashed lines, $n = 23$, penetrance = 100%). To determine whether dBRWD3 functions as a subunit of the CRL4 complex in these processes, we complemented *dBRWD3* mutant clones with either wild-type dBRWD3 or delta-N-dBRWD3 mutant proteins that cannot bind to the DDB1 adaptor of the CLR4 complex [24]. While expression of wild-type dBRWD3 restored the expression of Prospero (Fig 1D, dashed lines, $n = 69$, penetrance of restoration = 100%) and rescued the lethality of *dBRWD3* null mutants (Supplementary Table S1-1), expression of delta-N-dBRWD3 failed to do so (Fig 1E, $n = 27$, penetrance = 92.6%, and Supplementary Table S1-1), indicating that the binding to DDB1 in the CRL4 complex is essential for dBRWD3 to regulate gene expression and animal viability. It has been shown that CRL4B mediates the ubiquitination and subsequent degradation of WDR5, a core subunit of histone H3 lysine 4 (H3K4) methyltransferase complexes, thereby regulating the expression of neuronal genes [25]. However, H3K4me3 was not increased in *dBRWD3* mutant clones (Fig 1F, dashed lines, and G), suggesting that dBRWD3 regulates the development of photoreceptors and cone cells independently of WDR5.

Identification of *H3.3* as a suppressor of *dBRWD3*

To understand how dBRWD3 regulates photoreceptor differentiation, we conducted an RNAi screen to identify modifiers of the rough eye phenotype caused by knockdown of *dBRWD3* in the eye imaginal disk (*OK107-GAL4*-driven *UAS-dBRWD3-dsRNA*, Fig 2A). From the screen, we identified *H3.3B*, one of the two genes expressing H3.3, as a genetic suppressor. Double knockdown of *H3.3B* and *dBRWD3* restored normal eye development (Fig 2B). In contrast, *H3.3B* depletion alone did not cause any discernible eye abnormality (Fig 2C). This result prompted us to examine whether H3.3 levels are increased in *dBRWD3* mutant cells. Lacking a reliable antibody for immunofluorescence studies of endogenous H3.3, we analyzed the transgenically expressed dendra2-tagged H3.3 and found that H3.3-dendra2 levels were higher in *dBRWD3* mutant photoreceptors (Fig 2D, dashed lines) compared with those in wild-type twin spots. Western blot analysis confirmed an increase of both total and chromatin-associated endogenous H3.3 in *dBRWD3* mutants (Fig 2E; Supplementary Fig S1B). Taken together, we concluded that dBRWD3 negatively regulates the level of chromatin-associated H3.3. To examine whether the accumulated H3.3 caused abnormal gene expression, we knocked down H3.3 in *dBRWD3* mutant clones. The expression of Chaoptin (Fig 2F, arrows, $n = 44$, penetrance of derepression = 65.9%) and Prospero (Fig 2G, arrows, $n = 33$, penetrance of derepression = 84.8%) in posterior *dBRWD3* mutant clones increased when H3.3 was knocked down. Thus, the increased H3.3 also underlies the deregulation of gene expression in *dBRWD3* mutant clones. Because both *H3.3B* and *H3.3A* null mutants are viable [26,27], we were able to investigate the impact of reducing the number of *H3.3* copies on the viability of *dBRWD3* mutants. Strikingly, while all homozygous $dBRWD3^{PX2/PX2}$ mutant

Figure 1. *dBRWD3* is required for the differentiation of photoreceptors.
$dBRWD3^{s5349}$ mutant clones were generated in 3rd instar eye imaginal disks by *hs-flp* (A and F) or *ey-flp* (B to E) and marked by the presence (A, arrows) or the absence (B to F, dashed lines) of GFP. All scale bars indicate 50 μm. $dBRWD3^{s5349}$ mutant clones (B, C and E) were DAPI (blue) positive.

A Projection of axons from wild-type (Chaoptin positive) and $dBRWD3^{s5349}$ mutant photoreceptors (GFP positive, arrows) into the medulla layer of brain optic lobe.
B, C Expression of neuronal markers, Chaoptin (B), and Prospero (C) in wild-type (GFP positive) and $dBRWD3^{s5349}$ mutant photoreceptors (GFP negative, dashed lines).
D, E Prospero expression (red) in $dBRWD3^{s5349}$ mutant clones complemented with *Flag-dBRWD3* (D) and *Flag-delta-N-dBRWD3*, encoding a mutant dBRWD3 with a deletion of a conserved HLH-box ranging from amino acid 146 to 164 (E).
F Expression of H3K4me3 in wild-type (GFP positive) and $dBRWD3^{s5349}$ mutant photoreceptors (GFP negative, dashed lines).
G Quantification of H3K4me3 levels in wild-type and $dBRWD3^{s5349}$ mutant photoreceptors. $n = 39$, $P = 0.54$ by Student's *t*-test.

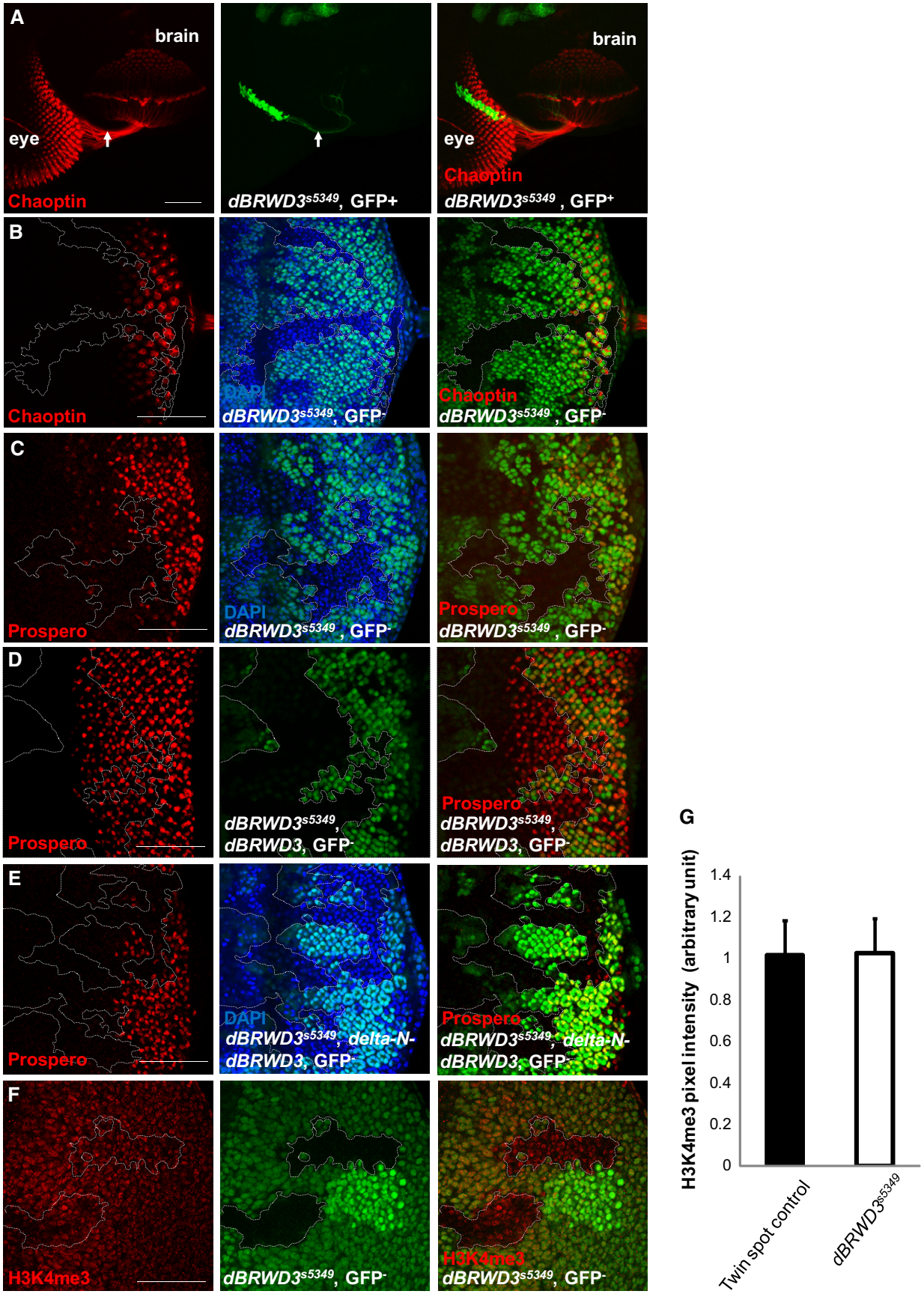

Figure 1.

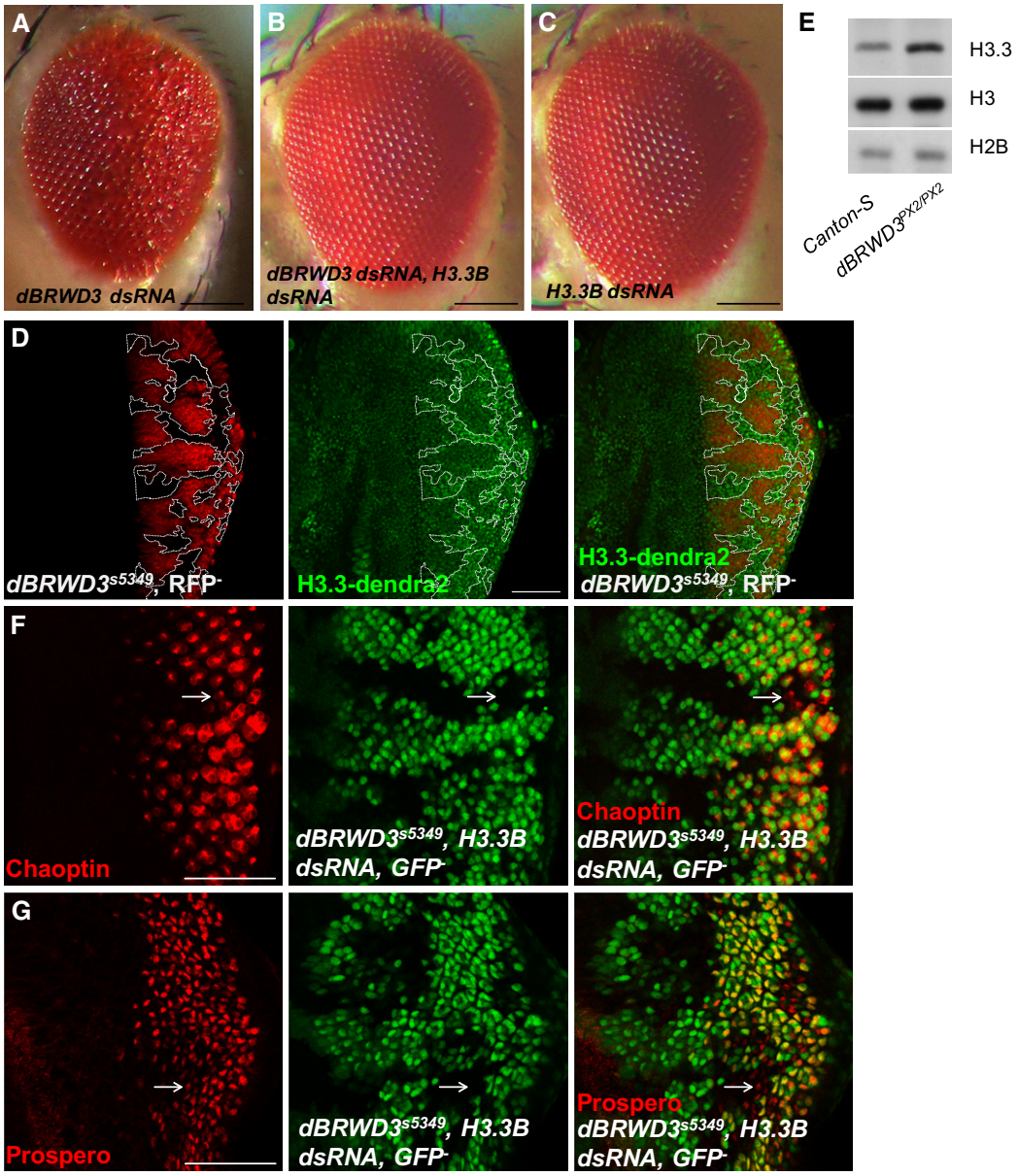

Figure 2. *dBRWD3* negatively regulates *H3.3*.

A–C Suppression of *dBRWD3-RNAi* induced rough eye phenotype by simultaneous *H3.3B* depletion. Images of adult eyes: *OK107-GAL4*-driven *UAS-dBRWD3-dsRNA* (A), *UAS-dBRWD3-dsRNA*, *UAS-H3.3B-dsRNA* (B), and *UAS-H3.3B-dsRNA* (C). Scale bars indicate 100 μm.

D The expression of *H3.3-dendra2* under the control of *ubi* promoter in 3rd instar $dBRWD3^{s5349}$ mutant clones generated by *ey-flp* (dashed lines, negatively marked by *GMR* promoter-driven RFP). The scale bar indicates 50 μm.

E Western blot analysis of endogenous H3.3 and total H3. Lysates prepared from *Canton S* and $dBRWD3^{PX2/PX2}$ 3rd instar larvae. The levels of endogenous H3.3 and total H3 were detected by Western blot analysis. Histone H2B was used as a loading control.

F, G Chaoptin (F) and Prospero (G) expression (red) in $dBRWD3^{s5349}$ mutant clones (arrows) expressing *GMR-GAL4*-driven *UAS-H3.3B-dsRNA*. Scale bars indicate 50 μm.

larvae died at the pupal stage, more than 40% of $H3.3B^{-/-}$, $dBRWD3^{PX2/PX2}$ mutants emerged as adults (Supplementary Table S1-2). Therefore, these data suggested that the increased H3.3 (likely the chromatin-associated H3.3, see below) contributes to the lethality of *dBRWD3* mutants. In other words, dBRWD3 is important for viability through controlling H3.3 levels. Consistently, over-expression of H3.3-GFP reduced viability in the otherwise viable transallelic, hypomorphic $dBRWD3^{06656/GS3279}$, but not in wild-type flies (Supplementary Table S1-3). Together, these findings indicate that dBRWD3, through its negative regulation of H3.3, is essential for gene expression and animal viability.

dBRWD3 depends on HIRA/YEM to regulate H3.3

Incorporation of H3.3 into chromatin is mediated by either the HIRA/YEM or Daxx/ATRX (Dlp/XNP in fly) complex [1,9,10]. We

therefore examined the functional relationship between dBRWD3 and the chaperones. Knockdown of *Hira* (Fig 3A) or *yem* (Fig 3B), but not *XNP* (Fig 3C), suppressed the rough eye phenotype caused by *dBRWD3* knockdown (Fig 3D). As a control, knockdown of *Hira* (Fig 3E), *yem* (Fig 3F) or *XNP* (Fig 3G) in a wild-type background did not result in any eye phenotype. These genetic analyses suggest that HIRA/YEM rather than Dlp/XNP complex may contribute to the increase of H3.3 levels in *dBRWD3* mutant cells. Consistently, in a co-immunoprecipitation experiment, Flag-tagged dBRWD3 pulled down Myc-tagged YEM as well as Myc-tagged HIRA, but not Myc-tagged XNP (Fig 3H). Domain mapping experiments revealed that HIRA directly or indirectly interacts extensively with dBRWD3 1-574a.a., 527-1214a.a., and 1049-1754a.a. fragments (Supplementary Fig S2A). In contrast, only the dBRWD3 1049-1754a.a. fragment directly or indirectly interacts with YEM (Supplementary Fig S2A). Within the dBRWD3 1049-1754a.a. fragment, bromodomain I is important since its deletion significantly reduced the interaction between dBRWD3 1049-1754a.a. and YEM (Supplementary Fig S2B).

The stabilization of H3.3 may be mediated either by its incorporation into chromatin or by blocking the rapid degradation of free H3.3. To identify which of the two processes is regulated by dBRWD3, we examined H3.3-dendra2 levels in *dBRWD3, yem* double mutant. The H3.3-dendra2 levels were similar to wild-type (Fig 3I, $n = 38$, penetrance = 100%), distinct from the marked increase of H3.3-dendra2 in *dBRWD3* mutant photoreceptors (Fig 2D). Consistently, both the total and chromatin-associated endogenous H3.3 increased only in the *dBRWD3* mutant, but not in the *dBRWD3*, *yem* double mutant (Fig 3J and K, $n = 3$, $P < 0.01$, and Supplementary Fig S1B), whereas non-chromatin-associated H3.3 appeared unchanged in *dBRWD3* mutant versus *dBRWD3*, *yem* double mutant (Supplementary Fig S1C). As a control, anti-H3.3 signal intensities increased linearly when the loaded chromatin fraction proteins increased (Supplementary Fig S1D). Independently, we also evaluated the ratio of chromatin-associated H3.3 to free H3.3 in salivary glands, where the exogenous, heat shock-inducible H3.3-GFP level in the control was about 70% of endogenous H3.3 (Supplementary Fig S1E) at 8 h after a 30-min heat shock. In a randomized, blind manner, we directly measured the GFP intensities that are colocalized (arrowheads in Supplementary Fig S1F and G) and non-overlapping (arrows in Supplementary Fig S1F and G) with DAPI as indexes for chromatin-associated and free H3.3, respectively (Supplementary Fig S1H). The analysis revealed an increase of chromatin-associated H3.3 relative to free H3.3 upon knockdown of *dBRWD3* (Supplementary Fig S1I), suggesting an increase of H3.3 chromatin association resulted from per unit of free protein. This increase was not because of a higher *H3.3-GFP* mRNA expression in *dBRWD3* knockdown salivary glands (Supplementary Fig S1J). Together, these data indicate that HIRA/YEM chaperone activity is required for the increased H3.3 observed in *dBRWD3* mutant cells. We therefore concluded that *dBRWD3* prevents an abnormal activation of HIRA/YEM, thus negatively regulating the amount of stable, chromatin-associated H3.3.

To next characterize the role of *dBRWD3* on the expression of histone chaperones, we performed knockdown of dBRWD3 in the S2 cells. As a control, the nuclear dBRWD3 protein level was significantly reduced after knockdown of *dBRWD3* (Supplementary Fig S3A). We next examined whether *dBRWD3* depletion caused increases of HIRA, YEM, and XNP by using Western blot analyses, which revealed that loss of *dBRWD3* did not change the levels of endogenous HIRA and XNP (Supplementary Fig S3B and C). In the case of YEM, although anti-YEM antibody detected overexpressed YEM well (Supplementary Fig S3D and E), it is not sensitive for endogenous YEM by either immunofluorescence or Western blot analyses (Supplementary Fig S3F and E, left panel). We therefore used an ectopic expression system—when *dBRWD3* was depleted in S2 cells stably expressing YEM-Myc, YEM-Myc protein levels also did not change (Supplementary Fig S3E, right panel). To further examine HIRA, YEM, and XNP protein levels in a *dBRWD3* null condition, we performed immunofluorescence studies in *dBRWD3* null mutant clones. Similarly, we found that endogenous HIRA and XNP levels were not altered in *dBRWD3* mutant clones (Supplementary Fig S3G and H), neither was endogenous YEM (Supplementary Fig S3I) nor the Flag-YEM (Supplementary Fig S3J) that faithfully recapitulates the expression pattern of endogenous YEM [5]. Together, we concluded that dBRWD3 regulates H3.3 levels in a manner independent of degradation of H3.3 chaperones, HIRA, YEM, and XNP. We next investigated whether dBRWD3 regulates the interaction between YEM chaperone and H3.3. There was a 2.3-fold increase of the YEM-associated HA-H3.3-RFP in *dBRWD3*-depleted S2 cells, compared with control (Fig 3L and M, left panel, $n = 4$). S2 cells were then treated with MLN4924 to test whether CRL4 ligase activity leads to the same outcome. As a control, MLN4924 treatment led to an increase in cullin substrate Armadillo (Supplementary Fig S3K). A similar 2.6-fold increase of HA-H3.3-RFP associated with Flag-YEM was observed (Fig 3L and M, right panel, $n = 4$), suggesting that dBRWD3-containing CRL4 E3 ligase negatively regulates the binding of Flag-YEM to HA-H3.3-RFP. The increased H3.3 binding of YEM upon the loss of *dBRWD3* is not due to an artifact of H3.3 overexpression as a similar increase was observed (Supplementary Fig S3M) in S2 cells stably expressing HA-H3.3-RFP at a much lower level than endogenous H3.3 (Supplementary Fig S3L, arrow and arrowhead). Moreover, we also observed a 2-fold increase of endogenous H4 associating with YEM in *dBRWD3*-depleted S2 cells (Supplementary Fig S3N).

Together, our data suggest that dBRWD3 interacts with HIRA/YEM either directly or indirectly and ubiquitinates an unidentified substrate to reduce the amount of H3.3 associated with YEM. This represents a new CRL4-mediated regulation of histone distinct from two previously reported mechanisms: ubiquitinations of H3 and H4 upon UV-induced DNA damage [28] and an ubiquitination of newly synthesized histone H3 at lysine 122 that moves H3.1 and H3.3 from ASF1 to CAF-1 and HIRA, respectively [29].

Inactivation of YEM suppresses lethality and aberrant gene expression caused by *dBRWD3* mutation

To investigate how much the aberrant HIRA/YEM activity contributes to *dBRWD3* mutant phenotypes, we first examined how well *dBRWD3*, *yem* double-mutant photoreceptors differentiated. The expression of neuronal differentiation markers Chaoptin (Fig 4A, dashed lines) and Prospero (Fig 4B, dashed lines) was restored to the wild-type level in the *dBRWD3, yem* double-mutant photoreceptors ($n = 31$ and $n = 22$ respectively, penetrance of restoration = 100%). In the adult stage, the number of surviving *dBRWD3* mutant ommatidia, as marked in red (*white*$^+$), is much smaller than wild-type twin spots marked in white (*white*$^-$) (Fig 4C, arrow). The

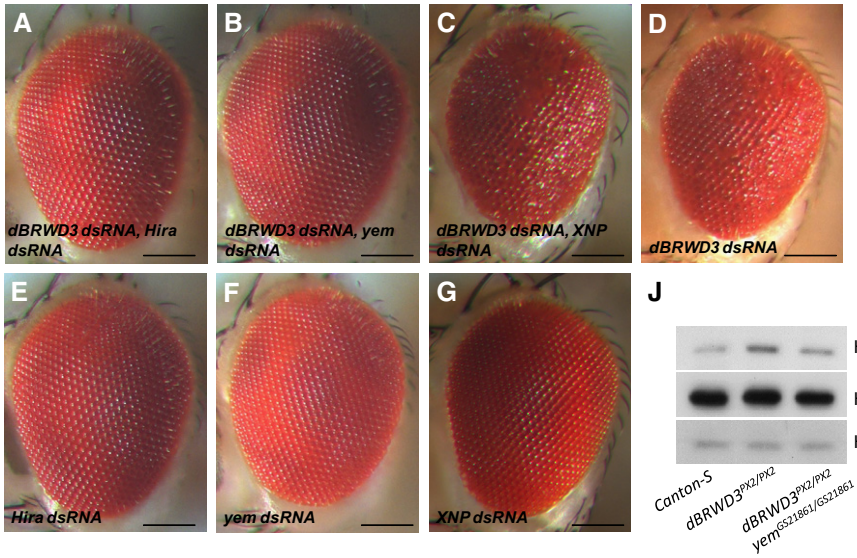

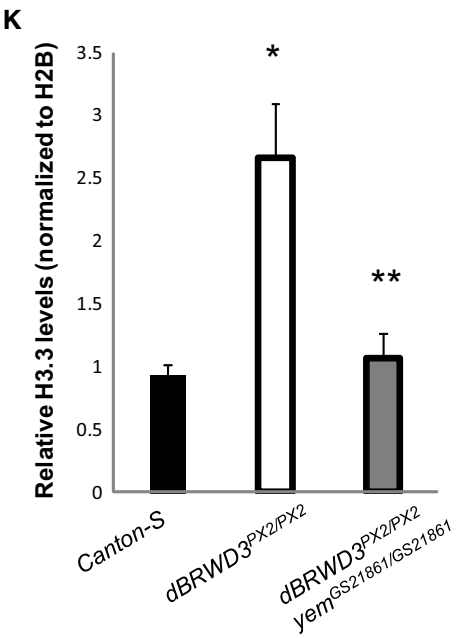

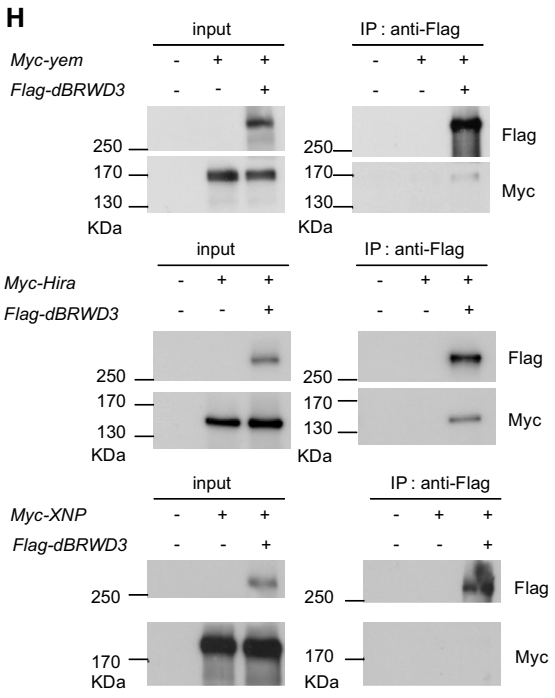

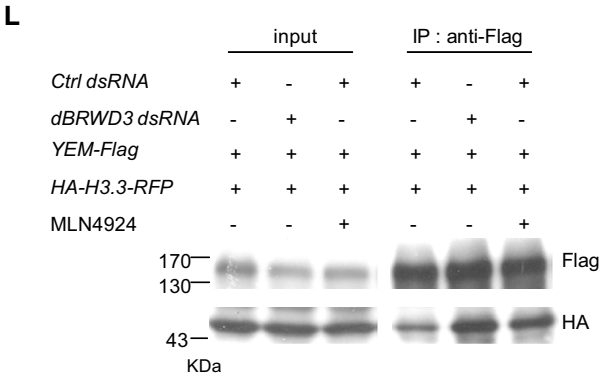

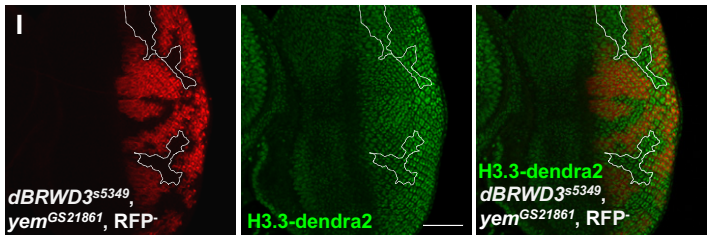

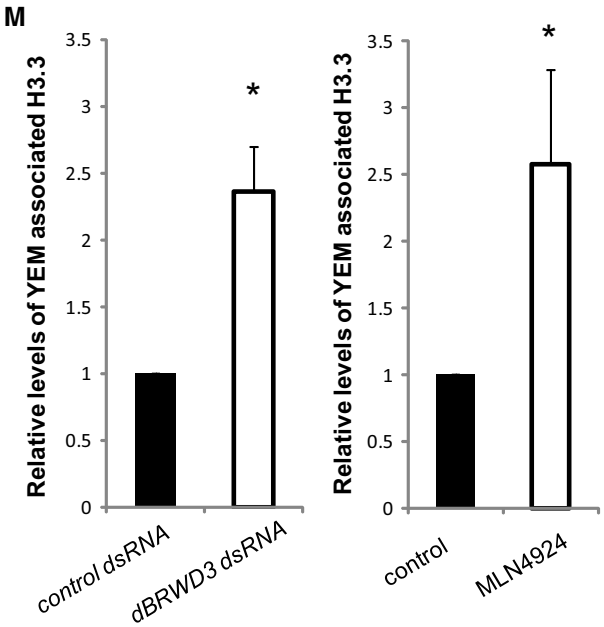

Figure 3.

Figure 3. dBRWD3 regulates H3.3 level in a HIRA/YEM-dependent mechanism.

A–G Suppression of *dBRWD3-RNAi* induced rough eye phenotype by simultaneous *Hira* or *yem* depletion. Images of adult eyes: *OK107-GAL4*-driven *UAS-dBRWD3-dsRNA*, *UAS-Hira-dsRNA* (A), *UAS-dBRWD3-dsRNA*, *UAS-yem-dsRNA* (B), *UAS-dBRWD3-dsRNA*, *UAS-XNP-dsRNA* (C), *UAS-dBRWD3-dsRNA* (D), *UAS-Hira-dsRNA* (E), *UAS-yem-dsRNA* (F), and *UAS-XNP-dsRNA* (G). Scale bars indicate 100 μm.

H Association of dBRWD3 with YEM, HIRA, and XNP. S2 cells were transfected with plasmids encoding Myc-tagged YEM (upper panel), Myc-tagged HIRA (middle panel), Myc-tagged XNP (lower panel), and Flag-tagged dBRWD3 as indicated. The expression of YEM, HIRA, XNP, and dBRWD3 were detected by Western blot analysis. dBRWD3 complex was immunopurified and analyzed by Western blot using anti-Myc antibody for the associated YEM (upper panel), HIRA (middle panel), and XNP (lower panel).

I Suppression of $dBRWD3^{s5349}$ by $yem^{GS21861}$ in the expression of *ubi-H3.3-dendra2*. Experimental settings similar to those in Figure 2D were applied to $dBRWD3^{s5349}$, $yem^{GS21861}$ mutants. Mutant photoreceptors are marked by the absence of RFP. The scale bar indicates 50 μm.

J Western blot analysis of endogenous H3.3 and total H3 in *Canton S*, $dBRWD3^{PX2/PX2}$, and $dBRWD3^{PX2/PX2}$ $yem^{GS21861/GS21861}$ 3rd instar larvae. H2B protein levels were included as a loading control.

K Quantification of endogenous H3.3 and total H3 in *Canton S*, $dBRWD3^{PX2/PX2}$, and $dBRWD3^{PX2/PX2}$ $yem^{GS21861/GS21861}$ 3rd instar larvae. Data shown were means ± SD from three independent experiments. *Indicates $P < 0.01$ versus *Canton S* and **indicates $P < 0.005$ versus $dBRWD3^{PX2/PX2}$ by Student's *t*-test.

L A representative Western analysis of YEM-associated H3.3. YEM-Flag and HA-H3.3-RFP were transiently expressed in control knockdown, *dBRWD3* knockdown, and MLN4924-treated S2 cells as indicated. The YEM-associated H3.3 was immunoprecipitated by anti-Flag antibody and analyzed by Western blot using anti-HA antibody.

M Quantification of YEM-associated H3.3 in *dBRWD3* knockdown (left panel) and MLN4924-treated (right panel) S2 cells. Data shown were means ± SD from four independent experiments. *Indicates $P < 0.01$ by Student's *t*-test.

number of *dBRWD3*, *yem* double-mutant ommatidia (red, Fig 4D, arrow) is similar to wild-type twin clones (white, Fig 4D), indicating that *dBRWD3*, *yem* double-mutant ommatidia are viable. Unlike *dBRWD3*, *yem* double mutant, the *XNP*, *dBRWD3* double-mutant clones (carrying a deletion allele of *XNP* [30], Fig 4E in red, arrow) are small, again suggesting dBRWD3 specifically regulates HIRA/YEM, but not Dlp/XNP. Like *H3.3B*, *dBRWD3* double mutant, the *dBRWD3*, *yem* double mutant could survive into the adult stage, whereas *dBRWD3* homozygous, *yem* heterozygous mutant could not (Supplementary Table S1-2), suggesting that *dBRWD3* is an essential gene to prevent an abnormal activation of HIRA/YEM. To determine whether dBRWD3 also regulates HIRA/YEM in other types of neurons, we performed transcriptome analyses on larval brains of *dBRWD3* heterozygous, *dBRWD3* homozygous, and *dBRWD3, yem* double homozygous mutants. Results from next-generation sequencing revealed that the expression of 871 genes was significantly different between heterozygous control and homozygous *dBRWD3* mutant brains (484 upregulated genes, 387 downregulated genes, $P < 0.05$) (Supplementary Table S2). Gene ontology (GO) analysis of the 871 genes revealed a broad spectrum of biological processes, ranging from synaptic activity to housekeeping metabolism, subjective to dBRWD3 regulation (Fig 4F, Supplementary Fig S4A). Among the 387 downregulated genes, the expression of 360 genes (92.8%) was increased in the *dBRWD3, yem* double-mutant brains compared with *dBRWD3* mutant. Among the 484 upregulated genes, the expression of 412 genes (85.1%) was decreased in the double-mutant brains (Fig 4F). These differentially expressed genes were evenly distributed on the X chromosome and autosomes (149 on X, 178 on 2L, 154 on 2R, 166 on 3L, and 207 on 3R), excluding the possibility of chromosome-specific regulation. These analyses indicate that dBRWD3 regulates gene expression in the brain mainly through the HIRA/YEM complex. Because the loss of *H3.3* restored the expression of Chaoptin and Prospero and viability in the *dBRWD3* mutant as the loss of *yem* did, we further investigated whether H3.3 also underlies the gene expression program regulated by dBRWD3 in brain. We examined 14 randomly chosen differentially expressed genes (seven upregulated, seven downregulated) in *Canton S*, *dBRWD3* null and *dBRWD3* null, *H3.3B* null double-mutant brains. Expression levels for 11 of the 14 chosen differentially expressed genes were significantly rescued in *dBRWD3* null, *H3.3B* null double-mutant brains (Fig 4G), suggesting that dBRWD3 regulates gene expression through H3.3 and HIRA/YEM. To further corroborate the notion, we examined H3.3 occupancy over 22 representative 100- to 110-bp regions, contributing 15% of total length of the seven randomly selected genomic regions. Chromatin immumoprecipitation analysis subsequently revealed a higher H3.3 occupancy on the 3′ end of *CG8664* and the gene body of *CG18765* (Supplementary Fig S4B), implying that *dBRWD3* regulates gene expression by limiting the H3.3 level on chromatin. The chromatin landscape in *Drosophila* can be divided into 9 distinct functional states according to the associated histone marks and epigenetic regulators [31]. To delineate the functional state of dBRWD3-associated chromatin, we examined the chromatin landscape features associated with genes that were upregulated and downregulated in *dBRWD3* mutant brains (Supplementary Fig S4C). The analysis revealed that active promoter/transcription start site regions, actively transcribed exons, actively transcribed introns (enhancers), other open chromatin, and actively transcribed exons on the male X chromosome (state 1–5) were overrepresented in upregulated genes, whereas actively transcribed introns (enhancers), other open chromatin, and actively transcribed exons on the male X chromosome and heterochromatin-like regions embedded in euchromatin (state 3–5 and 8) were enriched in the downregulated genes.

dBRWD3 has been implicated in complex cellular processes such as migration of Elav-positive nuclei and actin organization (Supplementary Fig S5) that require coordinated expression of many genes [23]. Given that most of the dysregulated genes in the *dBRWD3* mutant were rescued in *dBRWD3, yem* double mutants, we investigated whether the additional *yem* mutation could restore normal nuclear migration and actin cytoskeleton. Indeed, the *dBRWD3*, *yem* double mutant exhibited normal nuclei migration and actin organization (Supplementary Fig S5), indicating that HIRA/YEM chaperone activity underlies not only gene expression but also complex cellular processes, such as nuclear migration and cytoskeleton organization.

Inactivation of H3.3 reverses the diverse defects of the *dBRWD3* mutant nervous system

Among the 772 rescued differentially expressed genes, 349 genes (45.2%) were restored to levels comparable to control brains. Gene

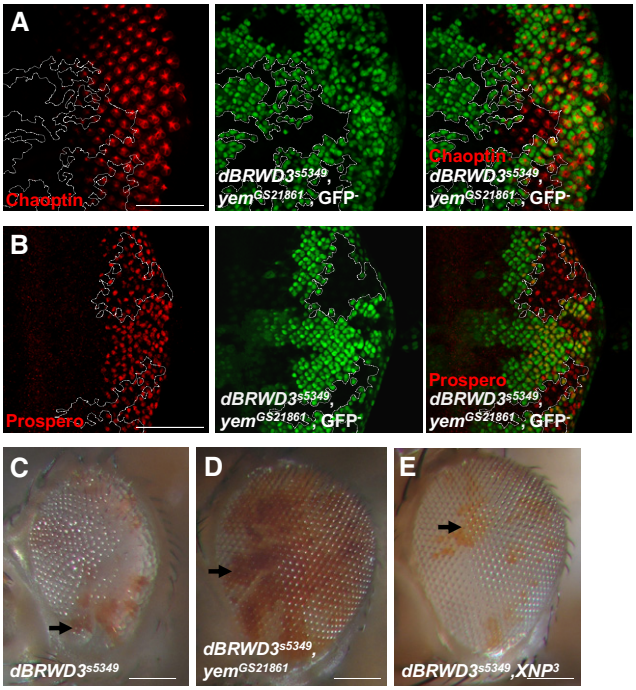

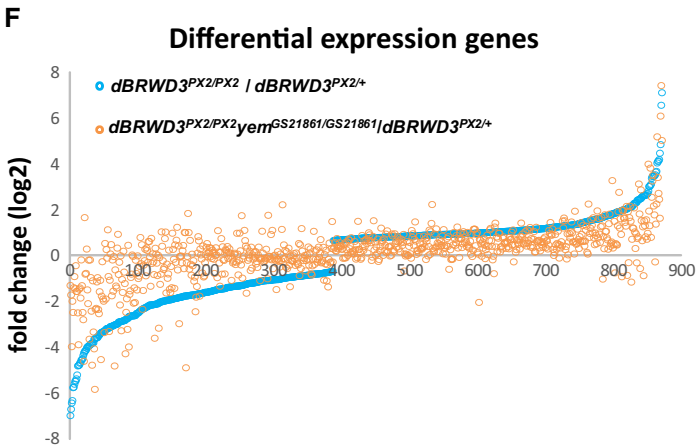

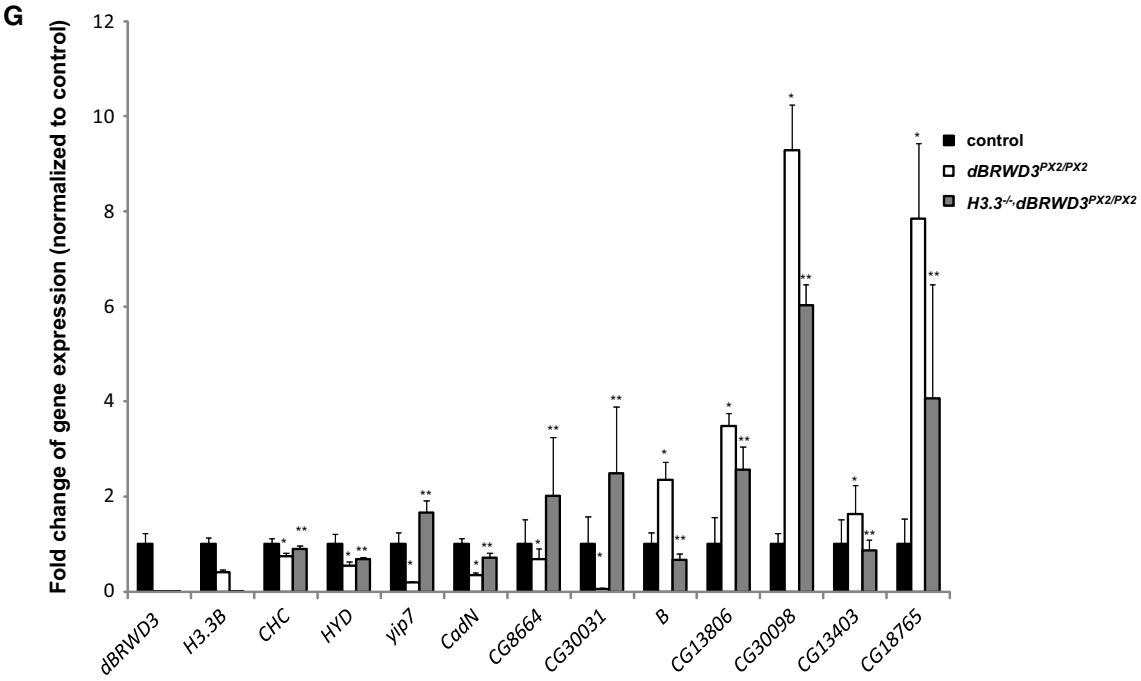

Figure 4. *yem* mutation suppresses *dBRWD3* mutant phenotypes.

A, B Expression of neuronal genes, Chaoptin (A), and Prospero (B) (red) in $dBRWD3^{s5349}$, $yem^{GS21861}$ mutant photoreceptors marked by the absence of GFP. Scale bars indicate 50 μm.

C–E Suppression of the cell lethality in adult $dBRWD3^{s5349}$ (null) clones by $yem^{GS21861}$. Adult homozygous $dBRWD3^{s5349}$ (C), $dBRWD3^{s5349}$, $yem^{GS21861}$ (D), and XNP^{3}, $dBRWD3^{s5349}$ (E) mutant photoreceptors were generated by *ey-flp* and marked by *white* gene expression (red regions, arrows), whereas wild-type twin clones were marked by the absence of *white* (white regions). Scale bars indicate 100 μm.

F Suppression of aberrant gene transcription in *dBRWD3* mutant brains by *yem* mutation. A scatter plot of the fold changes of the differentially expressed genes in $dBRWD3^{PX2/PX2}$ versus $dBRWD3^{PX2/+}$ brains shown in an increasing order (blue circles). The corresponding fold changes in $dBRWD3^{PX2/PX2}$, $yem^{GS21861/GS21861}$ versus $dBRWD3^{PX2/+}$ brains were shown as orange circles.

G Expression of the differentially expressed genes in $dBRWD3^{PX2/PX2}$ and $dBRWD3^{PX2/PX2}$, $H3.3B^{-/-}$ brains. The expression of *B*, *yip7*, *CadN*, *CG8664*, *CG13403*, *CG30031*, *CG13806*, *CG30098*, *CHC*, *HYD*, and *CG18765* in *Canton S*, $dBRWD3^{PX2/PX2}$ and $dBRWD3^{PX2/PX2}$, $H3.3B^{-/-}$ brains was analyzed by RT–PCR and presented as mean fold changes from 4 experiments relative to *Canton S* ± 1 SD. *Indicates $P < 0.05$ versus *Canton S* and **indicates $P < 0.05$ versus $dBRWD3^{PX2/PX2}$ by Student's *t*-test.

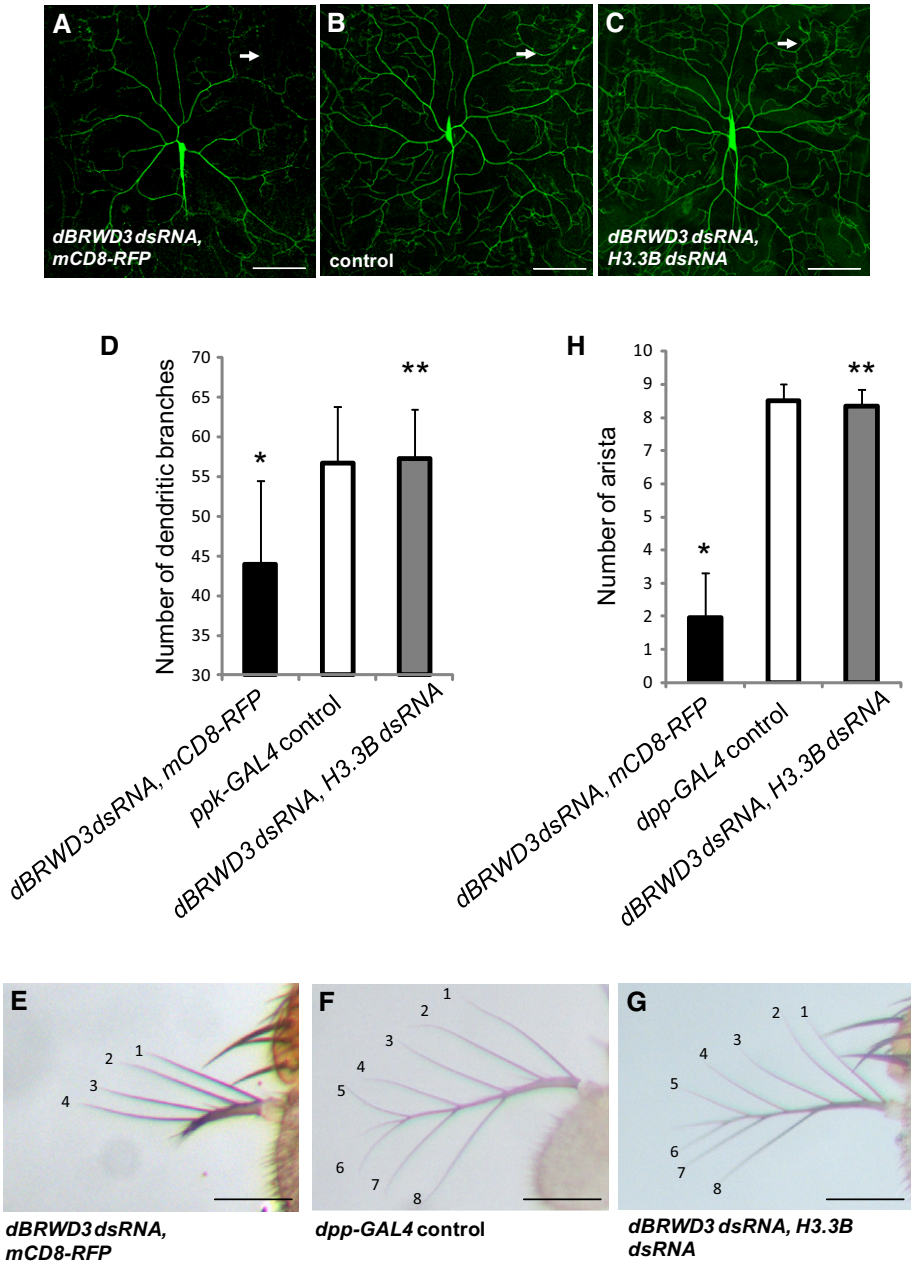

Figure 5. Knockdown of *H3.3* restores dendrite and arista development in *dBRWD3* knockdown flies.

A–D Dendrite morphogenesis regulated reciprocally by *dBRWD3* and *H3.3*. Dendrite morphogenesis of class IV da neuron was highlighted by *UAS-mCD8-GFP* driven by *ppk-GAL4*. (A) Specific knockdown of *dBRWD3* in class IV da neurons achieved by *ppk-GAL4*-driven *UAS-dBRWD3-dsRNA, UAS-mCD8-RFP* resulted in the absence of high-order dendritic branches (arrow). (B) High-order dendritic branches (arrow) increased in *ppk-GAL4*-driven *UAS-mCD8-GFP* control. (C) High-order dendritic branches (arrow) were restored in animals that simultaneously express *UAS-dBRWD3-dsRNA* and *UAS-H3.3B-dsRNA* by *ppk-GAL4*. (D) The mean dendritic branch number at 225 μm away from the soma from 27 independent experiments was shown. The error bars indicate 1 SD. *Indicates $P < 0.00001$ versus GAL4 control and **indicates $P < 0.00001$ versus *dBRWD3* knockdown by Student's *t*-test. Scale bars indicate 100 μm.

E–H Arista development is regulated by *dBRWD3* and *H3.3*. (E) Knockdown of *dBRWD3* in developing arista was achieved by *dpp-GAL4*-driven *UAS-dBRWD3-dsRNA, UAS-mCD8-RFP*. The number of branches and length were reduced in the *dBRWD3*-depleted arista. (F) Normal arista consists of 8–9 branches. (G) Both number of branches and length were restored in the *dBRWD3, H3.3B* doubly depleted arista. (H) The number of arista branches from 28 independent experiments was shown. The error bars indicate 1 SD. *indicates $P < 0.00001$ versus GAL4 control and **indicates $P < 0.00001$ versus *dBRWD3* knockdown by Mann–Whitney *U*-test. Scale bars indicate 100 μm.

ontology analysis revealed an enrichment of neuron-related terms, including dendrite morphogenesis and antenna development (Supplementary Fig S4D). Since reduced dendritic branching has been reported in ID such as Rett's syndrome [32], we next determined whether dBRWD3 affects dendritic morphogenesis through the negative regulation of H3.3. The *dBRWD3*-depleted class IV

dendritic arborization (da) sensory neurons had fewer dendritic branches (Fig 5A) compared with the control (Fig 5B), as judged by the number of dendritic branches at the periphery of the dendritic field (Fig 5D). But the dendritic branches were restored in *dBRWD3, H3.3B* doubly depleted da neurons (Fig 5C and D), supporting the notion that dBRWD3 regulates dendritic morphogenesis through the control of H3.3 levels. Similarly, the development of aristae, one of the two olfactory sensory organs in adult flies, was impaired in *dBRWD3*-depleted animals (Fig 5E) compared with the control (Fig 5F), but was restored to normal in *dBRWD3, H3.3* doubly depleted animals (Fig 5G and H).

Conclusion

In the present study, we show that dBRWD3 regulates gene expression in the developing nervous system and viability by limiting HIRA/YEM activity to control the levels of chromatin-associated H3.3, highlighting the fact that replication-independent nucleosome assembly needs to be tightly regulated. We also show that identifying the cause underlying the complex consequences associated with *dBRWD3* mutation by suppressor screening is rewarding: Inactivation of single HIRA/YEM–H3.3 pathway suppresses various complex *dBRWD3* mutant phenotypes, even global gene expression and viability. The HIRA/histone H3.3 pathway might thus represent an attractive therapeutic target for ID patients with *BRWD3* mutations.

Materials and Methods

Constructs

C-terminal Flag-tagged *dBRWD3, dBRWD3, dBRWD3* fragments, *yem, HA-yem*, *XNP* were amplified by PCR from the cDNA clones (*dBRWD3*: LD40380, *yem*: RE33235 and *XNP*: LD28477, Drosophila Genetic Resource Center). *delta-N-dBRWD3* lacking the region encoding amino acid 146 to 164 was generated by Thermo Scientific™ Phusion™ Site-Directed Mutagenesis kit. PCR products were cloned into *p-ENTR-D-TOPO* vector (Invitrogen). *pENTR-dBRWD3*, *pENTR-dBRWD3-Flag*, *pENTR-delta-N-dBRWD3,* and *pENTR-yem* were recombined into the *pUWR* vector (DGRC Gateway collection) to generate RFP-tagged *dBRWD3*, C-terminal doubly Flag-, RFP-tagged *dBRWD3*, RFP-tagged *delta-N-dBRWD3,* and RFP-tagged *yem*. All *pENTR-dBRWD3* fragments or deletion mutants were recombined into the *pAWF* vector (DGRC Gateway collection) to generate Flag-tagged dBRWD3 fragments or deletion mutants of dBRWD3 fragment (1049-1754a.a.). *pENTR-yem* was recombined into the *pAMW* vector to produce *pAMW-yem (Myc-yem)*. *pENTR-XNP* was recombined into the *pAMW* vector to produce *pAMW-XNP (Myc-XNP)*. *pENTR-HA-yem* was recombined into the *pTFW* vector to produce *HA-yem-Flag*. *Hira* and *H3.3B* CDS were PCR-amplified from cDNA, cloned into *p-ENTR-D-TOPO*, and recombined into the *pAMW* vector, the *pUWR* vector to produce *pAMW-Hira (Myc-Hira)*, *pUWR-HA-H3.3 (HA-H3.3-RFP)*, and *pUWR-H3.3-dendra2 (H3.3-dendra2)*.

Fly strains and genetics

Flies were raised in standard conditions at 25°C. The Canton S was used as wild-type control in all experiments. The $dBRWD3^{s5349}$, $dBRWD3^{PX2}$, and $dBRWD3^{06656}$ have been described earlier [23]. The $dBRWD3^{GS3279}$ allele is a transposable element insertion in the 3rd intron. The $yem^{GS21861}$ is a P-element insertion in the 2nd exon. Both $dBRWD3^{GS3279}$ and $yem^{GS21861}$ were obtained from Drosophila Genetic Resource Center, Kyoto. $dBRWD3^{s5349}$, $yem^{GS21861}$ double mutant was generated by recombination. *H3.3A* and *H3.3B* null mutant flies were generated and described by Dr. Hödl and Dr. Basler [26]. The heat shock-inducible *hs-H3.3-GFP* was a gift from Dr. Kami Ahmad [12]. The *UAS-Hira-dsRNA* (NIG12153R-1) was obtained from the Fly Stocks of the National Institute of Genetics, Kyoto, Japan (NIG-FLY). The *UAS-dBRWD3-dsRNA* (VDRC40209), *UAS-H3.3B-dsRNA* (VDRC12771), *UAS-yem-dsRNA* (VDRC26808), and *UAS-XNP-dsRNA* (VDRC101568) were obtained from the Vienna Drosophila RNAi Center (VDRC). *UAS-dBRWD3-dsRNA*, *UAS-H3.3B-dsRNA* was generated by recombination. *OK107-GAL4* was obtained from Drosophila Genetic Resource Center, Kyoto. *ppk-GAL4* has been described previously [33]. Other *GAL4* lines and XNP^3 [30] were obtained from Bloomington Drosophila Stock Center. The transgenic flies *ubi-dBRWD3-RFP, ubi-delta-N-dBRWD3-RFP, ubi-yem-RFP*, *ubi-HA-H3.3-RFP,* and *ubi-H3.3-dendra2* were generated by microinjection for germ line transformation. *ubi-H3.3-dendra2* contained the CDS of *H3.3B*. For expression of *hs-H3.3-GFP* in salivary glands, larvae were heat-shocked at 37°C for 30 min and dissected after 8 h.

Further details about clonal analysis, immunoprecipitation, Western blot, cell culture, transfection, RNA interference, immunostaining, RNA sequencing, transcriptome analysis, RNA extraction, reverse transcription, and real-time PCR can be found in the Supplementary Methods.

Open access of data

All RNA-sequencing data have been deposited in the NCBI Gene Expression Omnibus under accession number GSE64009.

Supplementary information for this article is available online: http://embor.embopress.org

Acknowledgements
We would like to acknowledge Dr. Moses in Wellcome Trust, Dr. Ahmad in Harvard University, Dr. Hödl and Dr. Basler in University of Zurich for sharing fly stocks. We thank Dr. CC Chan, Dr. HW Pi, Dr. ST Hsieh, Dr. TP Yao, Dr. CT Chien, Dr. RH Chen, Dr. Henikoff, Dr. Workman, and Dr. Abmayr for their suggestions. This work is supported by Career Development Grant to June-Tai Wu from National Health Research Institute, NSC 101-2321-B-002-062, and MOST 101-2321-B-002-082 grants from Ministry of Science and Technology, and Translational grants from National Taiwan University and National Taiwan University Hospital. We thank Taiwan Fly Core, fly core facility in National Taiwan University, and the sixth common core lab in National Taiwan University Hospital for their technical support.

Author contributions
W-YC, K-YL, H-TS, T-HT, and Z-SS carried out, analyzed, and interpreted the experiments. W-YC also participated in the writing of the article. L-KC, M-JC, C-YC, BC-MT, and HL performed RNA sequencing and analyzed RNA-sequencing data. H-HL, BL, OA-A, and J-TW designed experiments, interpreted data, and wrote the article. J-TW obtained the funding and carries the overall responsibility for the data.

Conflict of interest

The authors declare that they have no conflict of interest.

References

1. Tagami H, Ray-Gallet D, Almouzni G, Nakatani Y (2004) Histone H3.1 and H3.3 complexes mediate nucleosome assembly pathways dependent or independent of DNA synthesis. *Cell* 116: 51 – 61
2. Ray-Gallet D, *et al* (2011) Dynamics of histone H3 deposition in vivo reveal a nucleosome gap-filling mechanism for H3.3 to maintain chromatin integrity. *Mol Cell* 44: 928 – 941
3. Schneiderman JI, Orsi GA, Hughes KT, Loppin B, Ahmad K (2012) Nucleosome-depleted chromatin gaps recruit assembly factors for the H3.3 histone variant. *Proc Natl Acad Sci USA* 109: 19721 – 19726
4. Loppin B, Bonnefoy E, Anselme C, Laurencon A, Karr TL, Couble P (2005) The histone H3.3 chaperone HIRA is essential for chromatin assembly in the male pronucleus. *Nature* 437: 1386 – 1390
5. Orsi GA, *et al* (2013) Drosophila Yemanuclein and HIRA cooperate for de novo assembly of H3.3-containing nucleosomes in the male pronucleus. *PLoS Genet* 9: e1003285
6. Lin CJ, Koh FM, Wong P, Conti M, Ramalho-Santos M (2014) Hira-mediated h3.3 incorporation is required for DNA replication and ribosomal RNA transcription in the mouse zygote. *Dev Cell* 30: 268 – 279
7. Inoue A, Zhang Y (2014) Nucleosome assembly is required for nuclear pore complex assembly in mouse zygotes. *Nat Struct Mol Biol* 21: 609 – 616
8. Goldberg AD, *et al* (2010) Distinct factors control histone variant H3.3 localization at specific genomic regions. *Cell* 140: 678 – 691
9. Drane P, Ouararhni K, Depaux A, Shuaib M, Hamiche A (2010) The death-associated protein DAXX is a novel histone chaperone involved in the replication-independent deposition of H3.3. *Genes Dev* 24: 1253 – 1265
10. Lewis PW, Elsaesser SJ, Noh KM, Stadler SC, Allis CD (2010) Daxx is an H3.3-specific histone chaperone and cooperates with ATRX in replication-independent chromatin assembly at telomeres. *Proc Natl Acad Sci USA* 107: 14075 – 14080
11. Ng RK, Gurdon JB (2008) Epigenetic memory of an active gene state depends on histone H3.3 incorporation into chromatin in the absence of transcription. *Nat Cell Biol* 10: 102 – 109
12. Schwartz BE, Ahmad K (2005) Transcriptional activation triggers deposition and removal of the histone variant H3.3. *Genes Dev* 19: 804 – 814
13. Sarai N, Nimura K, Tamura T, Kanno T, Patel MC, Heightman TD, Ura K, Ozato K (2013) WHSC1 links transcription elongation to HIRA-mediated histone H3.3 deposition. *EMBO J* 32: 2392 – 2406
14. Ahmad K, Henikoff S (2002) The histone variant H3.3 marks active chromatin by replication-independent nucleosome assembly. *Mol Cell* 9: 1191 – 1200
15. Banaszynski LA, *et al* (2013) Hira-Dependent Histone H3.3 Deposition Facilitates PRC2 Recruitment at Developmental Loci in ES Cells. *Cell* 155: 107 – 120
16. Musante L, Ropers HH (2014) Genetics of recessive cognitive disorders. *Trends Genet* 30: 32 – 39
17. Bassani S, Zapata J, Gerosa L, Moretto E, Murru L, Passafaro M (2013) The neurobiology of X-linked intellectual disability. *Neuroscientist* 19: 541 – 552
18. Zou Y, *et al* (2007) Mutation in CUL4B, which encodes a member of cullin-RING ubiquitin ligase complex, causes X-linked mental retardation. *Am J Hum Genet* 80: 561 – 566
19. Tarpey PS, *et al* (2007) Mutations in CUL4B, which encodes a ubiquitin E3 ligase subunit, cause an X-linked mental retardation syndrome associated with aggressive outbursts, seizures, relative macrocephaly, central obesity, hypogonadism, pes cavus, and tremor. *Am J Hum Genet* 80: 345 – 352
20. Lee J, Zhou P (2012) Pathogenic Role of the CRL4 Ubiquitin Ligase in Human Disease. *Front Oncol* 2: 21
21. Field M, *et al* (2007) Mutations in the BRWD3 gene cause X-linked mental retardation associated with macrocephaly. *Am J Hum Genet* 81: 367 – 374
22. Grotto S, *et al* (2014) Clinical assessment of five patients with BRWD3 mutation at Xq21.1 gives further evidence for mild to moderate intellectual disability and macrocephaly. *Eur J Med Genet* 57: 200 – 206.
23. D'Costa A, Reifegerste R, Sierra S, Moses K (2006) The Drosophila ramshackle gene encodes a chromatin-associated protein required for cell morphology in the developing eye. *Mech Dev* 123: 591 – 604
24. Fischer ES, *et al* (2011) The molecular basis of CRL4DDB2/CSA ubiquitin ligase architecture, targeting, and activation. *Cell* 147: 1024 – 1039
25. Nakagawa T, Xiong Y (2011) X-linked mental retardation gene CUL4B targets ubiquitylation of H3K4 methyltransferase component WDR5 and regulates neuronal gene expression. *Mol Cell* 43: 381 – 391
26. Hodl M, Basler K (2009) Transcription in the absence of histone H3.3. *Curr Biol* 19: 1221 – 1226
27. Sakai A, Schwartz BE, Goldstein S, Ahmad K (2009) Transcriptional and developmental functions of the H3.3 histone variant in Drosophila. *Curr Biol* 19: 1816 – 1820
28. Wang H, Zhai L, Xu J, Joo HY, Jackson S, Erdjument-Bromage H, Tempst P, Xiong Y, Zhang Y (2006) Histone H3 and H4 ubiquitylation by the CUL4-DDB-ROC1 ubiquitin ligase facilitates cellular response to DNA damage. *Mol Cell* 22: 383 – 394
29. Han J, Zhang H, Wang Z, Zhou H, Zhang Z (2013) A Cul4 E3 ubiquitin ligase regulates histone hand-off during nucleosome assembly. *Cell* 155: 817 – 829
30. Bassett AR, Cooper SE, Ragab A, Travers AA (2008) The chromatin remodelling factor dATRX is involved in heterochromatin formation. *PLoS ONE* 3: e2099
31. Kharchenko PV, *et al* (2011) Comprehensive analysis of the chromatin landscape in Drosophila melanogaster. *Nature* 471: 480 – 485
32. Kaufmann WE, Moser HW (2000) Dendritic anomalies in disorders associated with mental retardation. *Cereb Cortex* 10: 981 – 991
33. Grueber WB, Ye B, Moore AW, Jan LY, Jan YN (2003) Dendrites of distinct classes of Drosophila sensory neurons show different capacities for homotypic repulsion. *Curr Biol* 13: 618 – 626

